

Article

Genome-Wide Analysis of the 12-Oxo-Phytodienoic Acid Reductase Gene Family in Peanut and Functional Characterization of *AhOPR6* in Salt Stress

Yifei Mou¹, Quanxi Sun¹ , Haocui Miao², Juan Wang¹, Qi Wang¹, Qianqian Wang¹, Caixia Yan¹, Cuiling Yuan¹, Xiaobo Zhao¹, Chunjuan Li¹ and Shihua Shan^{1,*}

¹ Shandong Peanut Research Institute, Qingdao 266100, China; yifeimou1123@163.com (Y.M.); squanxi@163.com (Q.S.); wangjuan_1984@163.com (J.W.); wqi0309@126.com (Q.W.); wangqianqian@saas.ac.cn (Q.W.); cxyan335@sina.com (C.Y.); yuanc1982@163.com (C.Y.); zhaoxiaoboqd@126.com (X.Z.); peanutlab@163.com (C.L.)

² Institute of Crop Germplasm Resource, Xinjiang Academy of Agricultural Sciences, Urumqi 830000, China; mc09876@163.com

* Correspondence: shansh1971@163.com

Abstract: 12-oxo-phytodienoic acid reductases (*OPRs*) have been substantiated as pivotal in plant growth and response to biotic and abiotic stresses. However, the functional characterization of *OPR* genes in the peanut genome remains limited. In this study, we identified a total of 20 *OPR* genes in a tetraploid cultivar and two diploid peanut species, categorizing them into two subfamilies, *OPRI* and *OPRII*. The gene structure and conserved protein motifs within each subfamily were elucidated. Additionally, our findings indicate an uneven chromosomal distribution of peanut *OPR* genes. Gene duplication events were identified as pivotal in the expansion of the *OPR* gene family. An analysis of cis-acting elements within *OPR* gene promoters revealed the presence of numerous phytohormone- and stress-related cis-elements. Furthermore, peanut *OPR* genes exhibited tissue-specific and stress-inducible expression patterns, underscoring their crucial role in peanut growth and stress response. Additionally, plants overexpressing *AhOPR6* exhibited significantly enhanced resistance to salt stress, and the *AhOPR6*-OE lines demonstrated a higher ability to scavenge reactive oxygen species (ROS). Collectively, these findings offer deeper insights into the roles of peanut *OPR* genes in stress responses, suggesting that *AhOPR6* could serve as a potential candidate gene for improving peanut salt tolerance through genetic transformation.

Keywords: peanut; 12-oxo-phytodienoic acid reductase; salt stress



Academic Editors: Ludovic Joseph Anatole Capo-Chichi and Jan Slaski

Received: 10 April 2025

Revised: 1 May 2025

Accepted: 6 May 2025

Published: 8 May 2025

Citation: Mou, Y.; Sun, Q.; Miao, H.; Wang, J.; Wang, Q.; Wang, Q.; Yan, C.; Yuan, C.; Zhao, X.; Li, C.; et al.

Genome-Wide Analysis of the 12-Oxo-Phytodienoic Acid Reductase Gene Family in Peanut and Functional Characterization of *AhOPR6* in Salt Stress. *Plants* **2025**, *14*, 1408. <https://doi.org/10.3390/plants14101408>

Copyright: © 2025 by the authors. Licensee MDPI, Basel, Switzerland. This article is an open access article distributed under the terms and conditions of the Creative Commons Attribution (CC BY) license (<https://creativecommons.org/licenses/by/4.0/>).

1. Introduction

The cultivated peanut, one of the most important economic oil crops worldwide, provides healthy oil and high-quality protein to the human diet, and it is used as animal feed [1]. Approximately 53% of the world's peanut production is used as high-quality edible oil, 32% is used for snack peanuts and candies, and about 15% is used as animal feed and in seed production [2]. Peanut plantation is widely carried out all over the world, from semi-arid tropical to subtropical regions [2,3]. The annual worldwide losses in peanut production as a result of various kinds of biotic and abiotic stresses equal approximately USD 3.2 billion [2]. Peanut is a moderately salt-tolerant crop [4]; planting peanut in saline-alkali areas could solve the urgent problem of the need to improve the utilization efficiency of saline-alkali land, which accounts for about 76% of the world's cultivated land area [5,6].

JA and related derivatives, namely *cis*-(+)-12-oxo-phytohormone jasmonic acid (*cis*-OPDA), methyl jasmonate (MeJA), and jasmonoyl-L-isoleucine (JA-Ile), participate in signal pathways in response to biotic and abiotic stresses, such as low temperature, hot stress, salinity tolerance, wounding, Hessian flies, aphids, and pathogens [7,8]. Besides contributing to the defense response, JA also acts in many plant growth and development processes, including tendril coiling, fruit ripening, pollen maturation, root growth, and seed germination [9,10]. JA biosynthesis mainly occurs in two organelles, chloroplasts and peroxisomes. JA biosynthesis starts from α -linolenic acid (LA) in chloroplast, which is then mediated by lipoxygenase (*LOX*), allene oxide synthase (*AOS*), and allene oxide cyclase (*AOC*) genes to generate 12-oxophytodienoic acid (OPDA) [11]. Afterward, the OPDA is transported into the peroxisome, where it is catalyzed by OPDA reductase (*OPR*) and reduced to 12-oxophytoenoic acid (OPC-8:0). Finally, the OPC-8:0 is converted to JA through three cycles of β -oxidation reaction [7].

12-oxo-phytodienoic acid reductases (*OPRs*) are the key precursors in the biosynthesis of jasmonic acid (JA), and they belong to the old yellow enzyme family (OYE), which contains flavin mononucleotide (FMN) as a non-covalently bound cofactor [12]. This family has several subfamilies in plants [13]. On the basis of the phylogenetic analysis of six green plant groups (green algae, mosses, lycophytes, gymnosperms, monocots, and dicots), *OPRs* can be divided into seven subfamilies. The *OPRs* in monocots are classified into five subfamilies (subs. I-V), while those in dicots are classified into two subfamilies (subs. I-II) [14,15]. In *Arabidopsis thaliana*, which belongs to the dicots, *OPR* can be divided into two groups (*OPRI* and *OPRII*) based on substrate specificity [16]. *AtOPRI1* and *AtOPRI2* (*OPRI*) enzymes preferentially catalyze (9R,13R)-12-oxophytodienoic acid (9R,13R-OPDA), and *AtOPRI3* (*OPRII*) can convert 9S,13S-OPDA to oxo-2(2'(Z)-pentenyl)-cyclopentane-1-octanoic acid (OPC-8:0) [14,17]. The classification of subfamilies III, IV, and V in rice (a monocot) was thoroughly explained by Li et al. (2011) [14]. The variable regions MVR i and MVR ii affect the three-dimensional (3D) structure of rice *OPR* proteins, which in turn influences the substrate specificity and catalytic activity of different subfamily proteins [14]. In rice, sub. I, sub. II, and sub. V have similar 3D structures, except in the MVR ii region. Sub. I and sub. II exhibit strong or moderate catalytic activity with substrates, while sub. V show weak catalytic activity. The distinction between sub. III and sub. IV, which have similar 3D structures, could be seen in MVR i [14].

To date, the identification of *OPR* genes has been performed in some dicots and monocots, such as *Arabidopsis* [17,18], rice [14], maize [19], tomato [20,21], and wheat [15]. The function of *OPRs*, which belong to subfamilies I and II in monocots (like rice, maize, and wheat) and dicots (*Arabidopsis*, tomato, and cotton), has been well documented; the *OPRs* participate in biotic and abiotic stress in diverse pathways [20,22–25]. In *Arabidopsis*, *AtOPRI1* and *AtOPRI2* were highly expressed in the roots and leaves [18], while *AtOPRI3* was detected in various tissues, especially in the flowers and anthers [26,27]. It has been reported that *OPRI* genes participate in some stress responses, such as stress caused by salinity, wounding, low temperatures, and pathogens. In wheat, overexpressing *TaOPRI1* (*OPRI*) could enhance salinity tolerance, and its heterologous expression in *Arabidopsis* promoted ABA synthesis and the ABA-dependent stress-responsive pathway [22]. *TaOPRI2* (*OPRII*), which is involved in the biosynthesis of JA in wheat, and the expression of *TaOPRI2* could be induced by wounding, drought, and methyl jasmonate (MeJA) [28]. Additionally, the expression of *TaOPRI2* increases after infection with *Puccinia striiformis* f. sp. *tritici* and *Puccinia recondita* f. sp. *tritici* [28]. In cotton, the transcripts of *AOS*, *AOC*, and *OPR*, along with the increased accumulation of α -linoleic acid, contribute to alleviating salt stress [29]. In rice, the *OsOPRI7* gene is crucial for JA synthesis, and *osOPRI7* mutants generated through CRISPR/Cas9 show male sterility with lower JA levels, which can be

recovered by exogenous MeJA [30]. In maize, the double mutant *OPR7OPR8* exhibited strong developmental defects, delayed leaf senescence, and increased susceptibility to insects and pathogens [23]. Significantly, in plants, only OPR II genes are related to the biosynthesis of JA. Due to the delayed anther filaments and inviable pollen grains, *OPR3* (OPR II subfamily) mutant plants are male sterile in *Arabidopsis*, and this phenotype can be restored by exogenous JA [26]. Silenced *OPR3* in tomato is more susceptible to the necrotrophic pathogen *Botrytis cinerea* and produces fewer seeds than the wild type (WT) [20]. Nevertheless, existing studies focus on the OPRI and OPRII subfamilies primarily in monocot plants and few dicots, and the potential functions of *OPR* genes in peanut remain unclear. Whether they possess a similar pathway in stress response still requires further validation in peanut.

In this study, all of the *OPR* genes in peanut (tetraploid cultivar peanut *Arachis hypogaea* “Tifrunner”, diploid *A. duranensis*, and *A. ipaensis*) were identified using the genome-wide analysis method. Then, the putative 20 *OPR* genes of peanut, 3 genes of *Arabidopsis*, and 10 genes of rice were used to construct a phylogenetic tree. The gene structure, protein conserved motifs, chromosomal locations, cis-acting elements in the promoter, gene duplication, gene ontology, and interactive networks were systematically investigated. Furthermore, the subcellular location of two *OPR* genes, *AhOPR3* and *AhOPR6*, was confirmed. One *OPR* gene (subfamily I) was cloned from the peanut cultivar Huayu71 and named *AhOPR6*. The overexpression of *AhOPR6* in *Arabidopsis* could enhance salt tolerance. The relative expression levels of twelve genes which related to JA and ABA signaling pathways were detected using qRT-PCR to understand the *OPRs*' potential functions in the ABA- or JA-dependent salt-responsive pathway. The findings of this study highlight the roles of peanut *OPR* genes in peanut growth and development. More importantly, we provide enough evidence that *AhOPR6* enhances salt stress tolerance and present a hypothetical model of *AhOPR6*'s action in improving salt tolerance.

2. Results

2.1. Identification and Analysis of Peanut *OPR* Genes

Based on the genomic databases of cultivated and wild-type peanut, 23 *OPR* genes were identified by the HMM profile of *OPR* (accession: PF00724). After confirming the *OPR* domain, it was found that 20 *OPR* genes have the whole domain, and they were used for the following investigation. The coding sequence length of peanut *OPRs* ranged from 339 (*AhOPR5*) to 573 (*AiOPR2*) amino acids. The molecular weights (MWs) of the *OPR* proteins ranged from 37.6 (*AhOPR5*) to 64.4 (*AiOPR2*) kDa, and the theoretical isoelectric points (pI) ranged from 5.52 (*AhOPR5*) to 7.15 (*AhOPR1*). The subcellular localization of most *OPR* proteins (15 out of 20) was predicted to be localized in chloroplast; *AdOPR4* and *AhOPR9* were localized in mitochondria. In addition, two *OPRs* (*AhOPR3* and *AiOPR3*) were predicted to be localized in plasma membrane. The predicted subcellular localizations of *OPRs* need further experimental validation. Detailed information of all of the above *OPR* genes, including the gene ID, protein length, molecular weight, theoretical pI, genomic location, and prediction of protein subcellular localization, is shown in Table S1.

2.2. Phylogenetic Analysis and Classification of *OPR* Gene Family

To investigate the evolutionary relationships of *OPRs*, a maximum likelihood phylogenetic tree (with 1000 bootstraps) was constructed using *Arabidopsis thaliana*, *Oryza sativa* L., and peanut (*Arachis ipaensis*, *Arachis duranensis*, and *Arachis hypogaea*) species. All *OPRs* could be classified into five subfamilies: OPR I, II, III, IV, and V (Figure 1). Twenty *OPRs* from three different peanut species could be divided into two subfamilies, OPR I and OPR II (Figure 1). The classification of peanut *OPRs* is similar to that of dicot plant *Arabidopsis*.

Among them, the OPR I subfamily contained the highest number of OPR proteins (16 out of 20; 80%), while OPR II contained four OPRs, including *AiOPR3*, *AdOPR4*, *AhOPR3*, and *AhOPR9*.

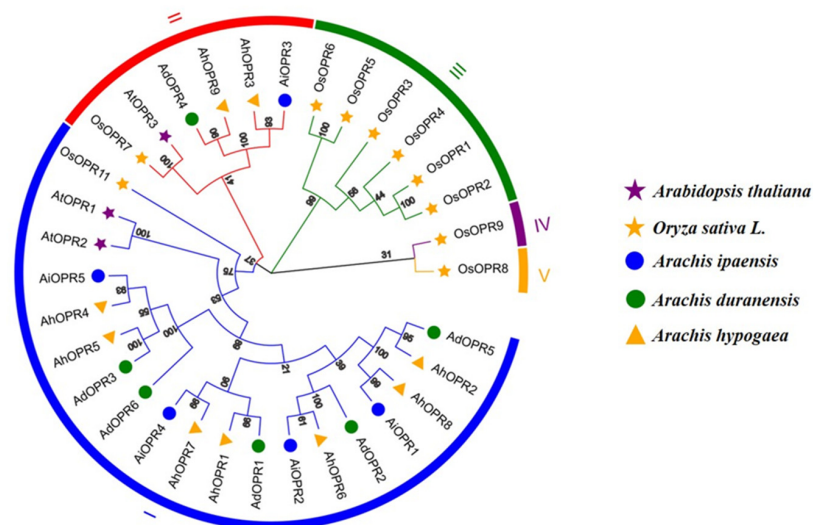


Figure 1. Phylogenetic tree of peanut OPR gene family members. Tree was constructed using neighbor-joining (NJ) method with peanut, rice, and Arabidopsis OPR proteins and bootstrap analysis with 1000 replicates.

2.3. Conserved Motifs and Gene Structure Analysis of Peanut OPR Genes

A maximum-likelihood phylogenetic tree (with 1000 bootstraps) was constructed using the multiple sequence alignment (ClustalW) of 20 conserved OPR proteins from peanut (Figure 2A). The MEME tool was used to identify the conserved motifs in peanut OPRs. At most, ten conserved motifs, with lengths between 6 and 50 amino acids, were found, showing diversity in each peanut OPR (Figure 2B, Table S2). In the OPR I and OPR II subfamilies, motifs 1–3, motif 5, and motif 7 were present in all OPRs, and they were the most conserved domains (Figure 2B). In *AiOPR3*, *AiOPR5*, and *AdOPR3*, the position of motif 9 was replaced by motif 4. Four OPRs in OPR II lacked motif 8, which was totally associated with the $\beta 6$ barrel of the protein secondary structures and further affected the 3D structure of *AhOPR3* and *AhOPR9* (Figure S1, Table S2). In the OPR I subfamily, *AhOPR4* and *AhOPR5* lacked motif 6, which reveals that they may have different functions (Figure 2B). Similar motifs in the same subfamily may have similar functions.

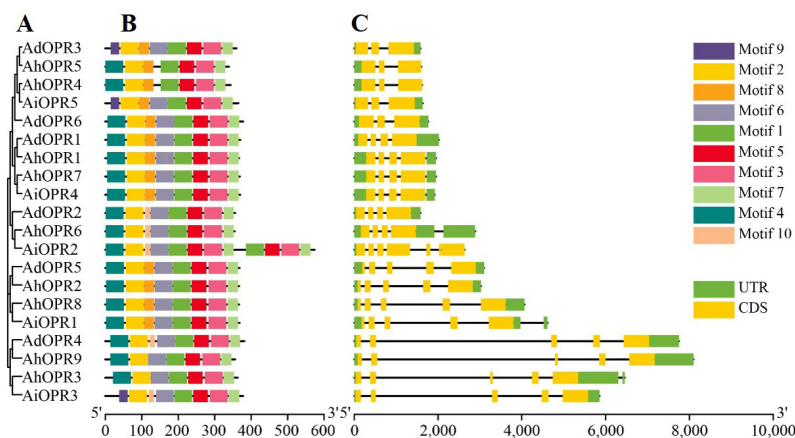


Figure 2. The phylogenetic relationship, gene structure, and protein conserved motif analysis of OPR genes in peanut. (A) The NJ phylogenetic tree with 1,000 replicates; (B) the conserved motifs of OPR proteins; (C) the gene structures (exon-intron) of OPR genes.

To further analyze the gene structure of peanut *OPR* genes, the gene structure features were exhibited by TBtoolsV1.098 (Figure 2C). As shown in Figure 2C, most *OPR*s of peanut contain 3–5 exons. *AiOPR2* contained the highest number of exon 7. In addition, we found that the intron numbers and lengths were diverse in different subfamilies (Figure 2C). All the genes in *OPR II* contained 4 introns, and the second intron was significantly longer than others compared with genes in the *OPR I* subfamily (Figure 2C). In *OPR I*, most *OPR*s (approximately 70%) had 2–3 introns, and the others contained more than 4 introns (Figure 2C).

2.4. Chromosomal Locations and Synteny Analysis of Peanut *OPR*s

A total of 20 peanut *OPR* genes were unevenly distributed on 40 chromosomes (Figure 3). No genes were found on 29 chromosomes, including chromosomes A1–4, A7, B1–4, B8, 1–4, 7, 9–14, and 18. The maximum number of *OPR* genes appeared in chromosome A5 (4, 20%), and the second largest number of *OPR* genes were found on chromosome B5 (3, 15%) and 15 (3, 15%). There was one gene on chromosomes A6, A8, B6, B7, 8, and 17 (Figure 3). Two *OPR* genes were mapped on chromosomes 5 and 16, respectively (Figure 3). To further study the gene duplication events of peanut *OPR* genes, tandem and segmental duplicated gene pairs were analyzed (Figure 4 and Table S3). There were two groups of tandem duplicated genes, including *AdOPR1* and *AdOPR2* and *AdOPR2* and *AdOPR6*, which were linked with red lines. In addition, 14 segmental duplication gene pairs are visualized in Figure 4. The number of segmental duplicated gene pairs was dramatically higher than the tandem duplicated gene pairs; this might be the main reason for the expansion of the *OPR* gene family.

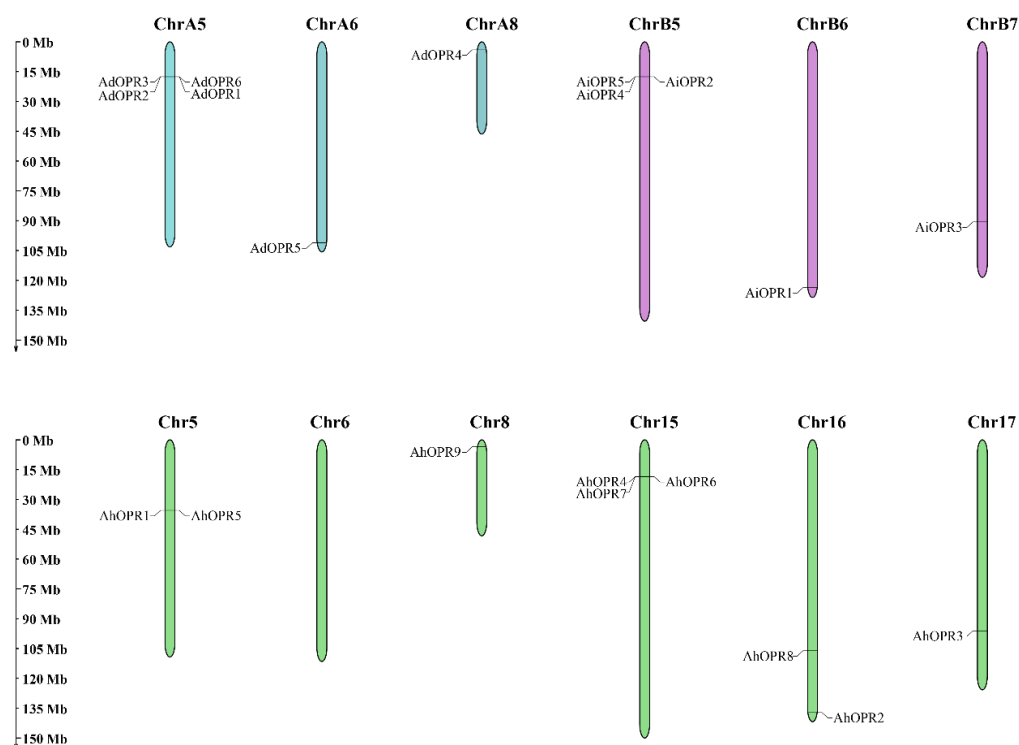


Figure 3. Chromosomal locations of *OPR* genes. Genes from different peanut species are shown in different colors (*Arachis duranensis*: blue, *Arachis ipaensis*: purple, and *Arachis hypogaea*: green).

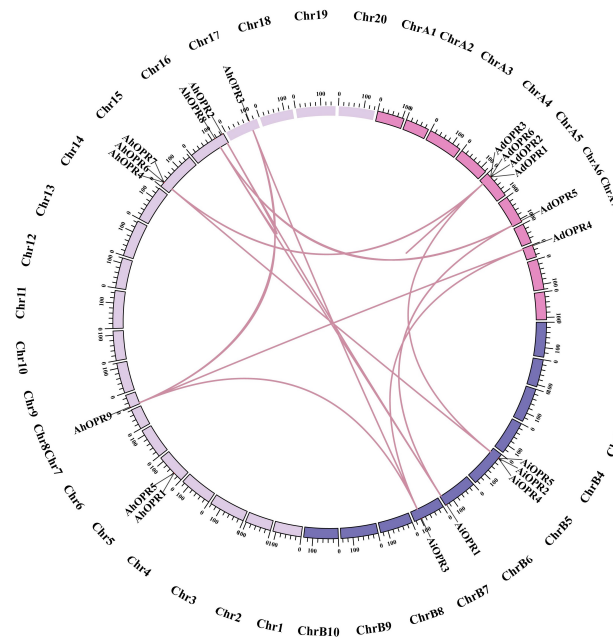


Figure 4. Synteny analysis of *OPR* genes in peanut. Lines highlighted in red indicate duplicated gene pairs of peanut *OPR* genes.

2.5. Prediction and Analysis of Cis-Acting Elements in Promoter Sequences of OPR Genes

To further explore the evolution and functional characterization of peanut *OPR* genes, the 1.5 kb areas upstream from the translational start site of each gene were analyzed. Various cis-acting elements were found in *OPR* promoters (Table S4). As shown in Figure 5, peanut *OPR* promoters contained elements associated with endosperm development, meristem development, light, GA, ABA, SA, MeJA, auxin, drought, zein metabolism, low-temperature, circadian, anaerobic, and defense stresses. The cis-acting elements (Box 4, ATCT-motif, Box II, AAAC-motif, ATC-motif, GT1-motif, GATA-motif, I-box, GA-motif, G-Box, and TCT-motif) related to light were all found in the *OPR* gene promoter. The majority of the *OPR*s included elements responsive to ABA (ABRE), SA (TCA-element), and MeJA (TGACG-motif and CGTCA-motif) (Figure 5). A small number of gene promoters were identified to be involved in responses to drought (MBS), GA (GARE-motif and P-box), auxin (TGA-element), low-temperature (LTR), anaerobic (ARE), and defense stresses (TC-rich repeats). These findings indicated that peanut *OPR* genes might participate in plant growth and development and the response to hormones and diverse stresses.

	AAAC-motif	GC-box	GAT-box	Box 4	ATCT-motif	Box II	AAAC-motif	ATC-motif	TCCC-motif	NTI-motif	GT1-motif	GATA-motif	I-box	MRE	GA-motif	G-box	TCT-motif	GARE-motif	P-box	ABRE	TCA-element	TGACG-motif	CGTCA-motif	TGA-element	MBS	O2-site	circadian	defense and stress	TC-rich repeats
AdOPR1	0	0	0	9	1	0	0	0	1	1	0	0	0	0	0	2	0	0	0	0	0	0	0	0	0	0	0	0	
AdOPR2	0	1	1	9	0	0	0	0	0	0	0	0	0	1	1	2	1	0	0	2	0	3	3	0	1	0	0	0	
AdOPR3	0	0	0	10	0	0	0	0	0	0	0	0	0	0	0	0	0	1	0	0	1	2	2	0	0	1	0	2	
AdOPR4	0	0	0	7	1	0	0	1	0	0	0	0	0	0	0	0	1	0	0	0	1	0	0	1	0	0	0	0	
AdOPR5	0	0	0	3	0	0	0	0	0	0	0	2	0	1	1	1	0	0	0	0	0	0	0	1	0	2	1	0	
AdOPR6	0	0	1	0	0	1	1	0	0	0	1	1	1	0	1	0	1	0	1	2	0	0	2	0	0	1	0	2	
AhOPR1	0	0	0	8	1	0	0	0	1	0	0	0	0	0	0	3	0	0	0	1	0	1	1	0	0	0	0	0	
AhOPR2	0	0	1	4	0	0	0	0	0	0	4	0	0	1	0	0	0	0	0	0	0	0	0	1	0	2	1	0	
AhOPR3	0	0	0	9	2	0	0	0	0	0	1	0	0	0	0	0	2	0	0	0	2	0	0	0	1	0	0	0	
AhOPR4	0	0	0	5	0	0	0	0	0	0	0	0	0	2	0	0	1	0	1	0	2	3	3	0	0	0	0	1	
AhOPR5	0	0	0	9	0	0	0	0	0	0	0	0	0	0	0	0	1	0	0	0	2	1	1	0	0	0	0	1	
AhOPR6	1	1	0	6	0	0	0	0	0	1	0	0	0	0	1	1	2	0	0	1	1	1	1	0	2	0	0	0	
AhOPR7	0	0	0	8	0	0	0	0	0	2	0	0	0	0	0	3	0	0	0	2	0	3	3	0	0	0	0	0	
AhOPR8	0	0	0	7	0	0	0	0	0	1	0	0	0	2	0	2	1	0	0	1	3	0	2	2	4	0	2	1	
AhOPR9	0	0	0	7	1	0	0	1	0	0	0	0	0	0	0	0	1	0	0	0	1	0	0	0	1	0	0	0	
AiOPR1	0	0	0	6	0	0	0	0	0	1	0	0	0	2	0	2	1	0	0	1	3	0	2	2	5	0	2	1	
AiOPR2	1	1	0	7	0	0	0	0	0	1	0	0	0	0	1	1	2	0	0	0	1	1	1	1	0	2	0	0	
AiOPR3	0	0	0	10	0	0	0	0	0	2	0	1	0	1	0	2	0	0	0	2	2	1	1	1	0	1	1	0	
AiOPR4	0	0	0	5	0	0	0	0	0	5	0	0	0	1	0	0	1	0	0	1	0	4	4	0	0	0	0	2	
AiOPR5	0	0	0	3	0	0	0	0	0	0	0	0	0	3	0	0	1	0	0	0	1	3	3	0	0	1	0	1	

Figure 5. Cis-acting element analysis in promoter regions of peanut *OPR* genes.

2.6. Expression Patterns of OPR Genes in Different Tissues and in Response to Various Stresses

To gain more insights into the temporal and spatial expression patterns of OPR genes, the RNA sequences of different treatments under abiotic stress (Table S5) and 22 tissues (Table S6) were analyzed. Most genes exhibited different expression levels across 22 tissues (Figure 6A). The results show that four genes had relatively high expression levels in all 22 tissues, while three genes had relatively low expression levels in all 22 tissues (Figure 6A). Some peanut OPR genes exhibited tissue-specific expression patterns, such as *AhOPR4* and *AiOPR5*, which were prominently expressed in flowers. Additionally, *AdOPR4*, *AhOPR3*, *AhOPR9*, and *AiOPR3* displayed specific expression in the seeds.

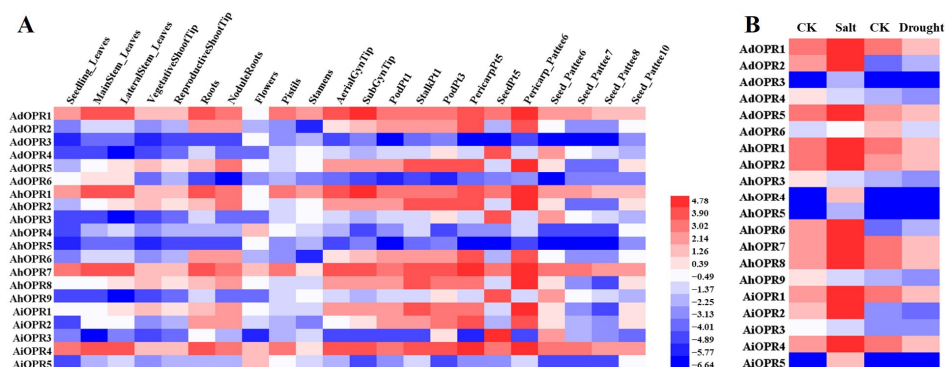


Figure 6. Expression profiles of OPR genes in 22 different tissues and stress conditions. (A) Heatmap of OPR family genes in 22 peanut tissues; (B) heatmap of OPR family genes under salt and drought treatments. Fragments per kilobase of transcript per million fragments (FPKM) of peanut OPR genes were log₂-transformed using Heml_1.0 software.

The expression levels of the genes under drought and salt stresses were investigated using our published transcriptome sequencing results. We found that the expression pattern of peanut OPRs was notably different under drought and salt stresses. In Figure 6B, the expression of most peanut OPRs (16 of 20) was upregulated by more than 2-fold under salt stress, and the majority of OPRs were increased by up to 10-fold. Unlike salt treatment, only three OPRs (*AdOPR2*, *AhOPR6*, and *AiOPR3*) were upregulated under drought stress, and the majority OPR genes were downregulated. It is worth noting that the expression of four OPR genes (*AdOPR3*, *AhOPR4*, *AhOPR5*, and *AiOPR5*) was unchanged in response to drought stress. Only two genes (*AdOPR2* and *AhOPR6*) were upregulated both under salt and drought stresses, and the *AhOPR6* gene was selected for further functional study.

2.7. Subcellular Location of Peanut OPR Proteins

AhOPR proteins were predicted to be localized in the chloroplast, plasma membrane, or mitochondria using the online web tool WoLF PSORT (Table S1). In order to confirm the subcellular localization of the peanut proteins, *AhOPR3* and *AhOPR6* proteins were selected to perform the experiment (Figure 7). The 35S::*AhOPR3*-GFP and 35S::*AhOPR6*-GFP fusion proteins were constructed, together with 35S::GFP (the empty vector), and they were transiently expressed in *N. benthamiana*. Confocal microscopy observations revealed that the green fluorescence of the empty vector was found in the cytoplasm and on the plasma membranes, while the 35S::*AhOPR3*-GFP fusion protein was distributed on the plasma membranes, and the 35S::*AhOPR6*-GFP fusion proteins was localized in the chloroplast (Figure 7).

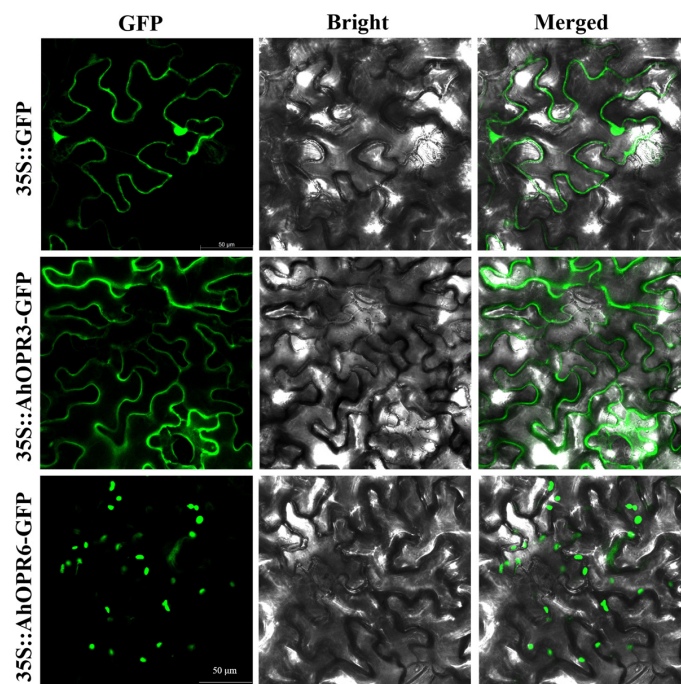


Figure 7. The subcellular localization of *AhOPR3* and *AhOPR6* proteins. The *AhOPR3*-GFP, *AhOPR6*-GFP fusion protein, and GFP protein were transiently expressed into tobacco epidermal cells. Bar = 50 μ m.

2.8. Gene Ontology (GO) and Interactive Networks of Peanut OPR Genes

GO analysis offers valuable information for investigating potential associations based on their enrichment in molecular function (MF), cellular components (CCs), and biological process (BP). This analytical tool is commonly used in genetics to validate the functions of candidate genes. As shown in Figure 8A, all peanut *OPR*s were significantly enriched to allene oxide cyclase activity (MF), FMN binding (MF), the oxylipin biosynthetic process (BP), the jasmonic acid (JA) biosynthetic process (BP), and the oxylipin metabolic process (BP). All *OPR* genes were found to be associated with allene oxide cyclase activity, the oxylipin biosynthetic process, and FMN binding (Figure 8B). A further annotation analysis of *AhOPR*s using data from ShingGO confirmed a tree of three clusters according to a correlation analysis (Figure 8C).

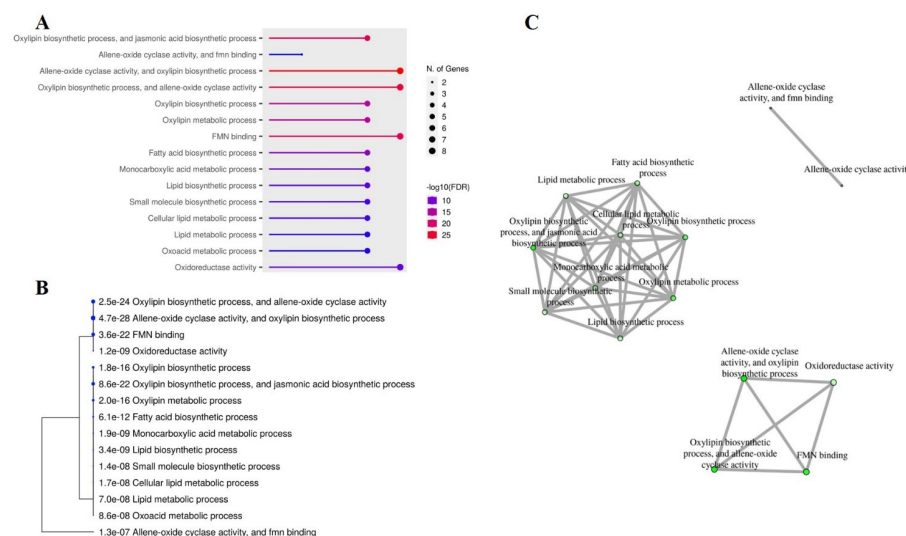


Figure 8. Analysis of gene ontology (GO) and interactive enrichment networks in ShinyGO database. (A) GO of *AhOPR6* genes; (B) phylogenetic analysis of *AhOPR6* gene annotations; (C) interactive enrichment networks of *AhOPR6* genes.

2.9. Overexpression of *AhOPR6* Enhanced Salt Tolerance in Seedlings

To further explore the function of the *OPR* genes in salt response, overexpressing *AhOPR6* transgenic plants were investigated. Overall, twenty T0 transgenic lines were obtained by PCR using *Arabidopsis* genomic DNA. After cultivation and screening, the homozygous T3 transgenic lines of *AhOPR6* were used to analyze the functional roles in salt stress. After being treated with 300 mM of NaCl for one week, most leaves of the wild-type plants were wilted, while only a small number of OE1 and OE2 leaves became wilted (Figure 9A). Furthermore, the activities of SOD (Figure 9B), POD (Figure 9C), and CAT (Figure 9D) enzymes associated with ROS scavenging were increased after salt stress, and gene-overexpressed plants were obviously increased in SOD, POD, and CAT activity compared with wild-type *Arabidopsis*. Before the salt treatment, the wild-type and transgenic *Arabidopsis* lines had nearly equal MDA contents (Figure 9E). Transgenic *Arabidopsis* lines have significantly lower MDA contents after salt treatment (Figure 9E). These results reveal that the overexpression of the peanut *AhOPR6* gene enhanced salt tolerance in *Arabidopsis*.

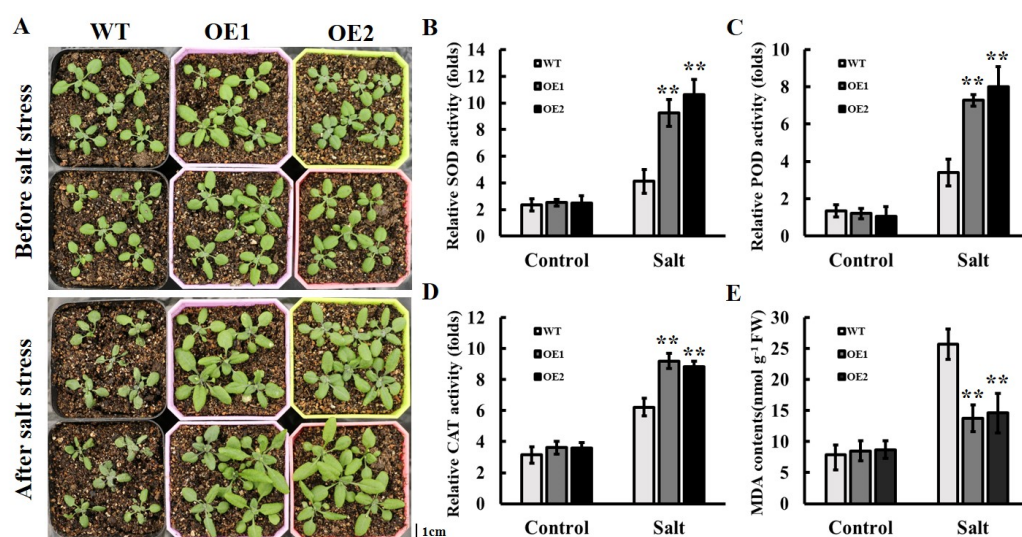


Figure 9. Overexpression of *AhOPR6* enhanced salt tolerance in *Arabidopsis*. (A) Phenotype of wild-type (WT) and OE lines with and without salt treatment. Bar = 1 cm. SOD (B), POD (C), and CAT (D) activities of overexpressing lines and WT *Arabidopsis* after salt stress. (E) MDA contents. Data are shown as means \pm SD from three independent replications. ** $p < 0.01$ (t -tests).

2.10. The Overexpression of *AhOPR6* in *Arabidopsis* Affects the Expression of JA/ABA Pathway-Related Genes

To further validate the role of ABA- and JA-related genes in *AhOPR6*-mediated salinity stress enhancement, the transcript abundance of 12 genes was monitored (Figure 10, Table S7). Some genes, like *AtAAO*, *AtNCED*, *AtRD*, *AtMYB*, and *AtMYC*, were key factors in the ABA-dependent stress-responsive signaling pathway; *AtAOC*, *AtOPR*, and *AtJAZ* were all key components of the JA biosynthesis pathway in *Arabidopsis*. The transcript abundance of *AtAAO3* and *AtNCED3* was increased in the *AtOE-AhOPR6* lines; *AtRD22*, *AtRD29A*, and *AtRD29B* were also upregulated in the *AhOPR6*-overexpressing *AtOE* lines (Figure 10). The expression levels of two upstream transcription factors, *AtMYB2* and *AtMYC2*, were significantly upregulated as expected. In the JA synthesis pathway, the expression levels of *AtAOC1*, *AtOPR1*, *AtOPR2*, and *AtJAZ1* were significantly upregulated in transgenic *Arabidopsis* lines, while the expression of *AtOPR3* was not influenced by the overexpression of peanut *AhOPR6*.

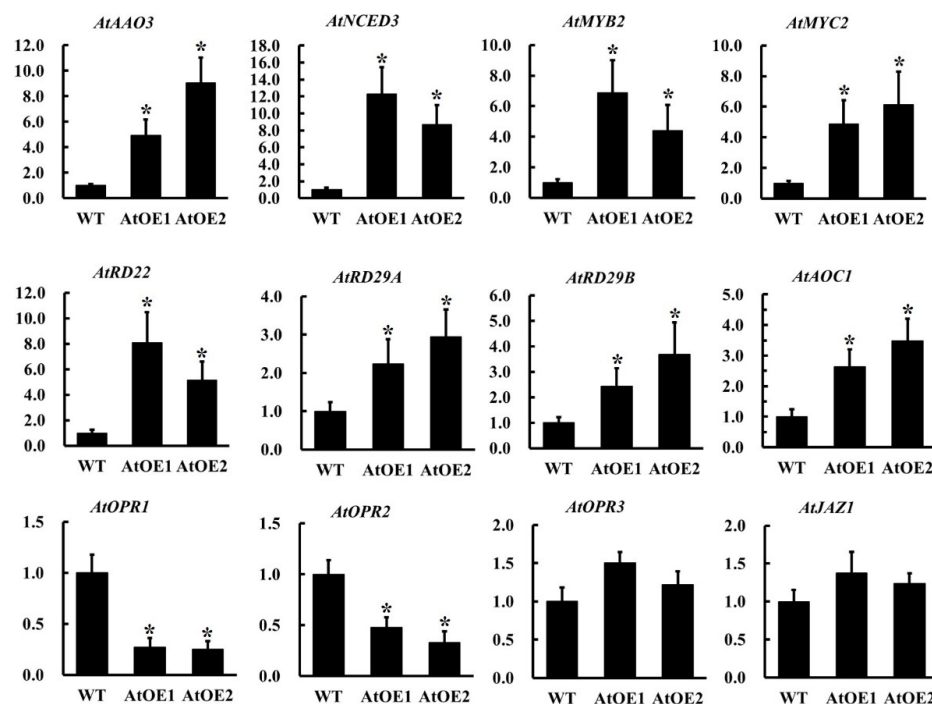


Figure 10. The relative expression level of JA/ABA pathway-related genes in the WT and OE lines of *Arabidopsis*. The data are shown as the means \pm SD from three independent replications. * $p < 0.05$ (t -tests).

3. Discussion

Peanut is an important economic and oil crop worldwide. However, annual worldwide losses caused by various biotic and abiotic stresses are destructive. The objective of this study was to explore all the OPRs in peanut and the potential role of OPRs in peanuts' resistance. OPRs are key enzymes that participate in the last step of JA synthesis. JA and its derivatives regulate the development and response to biotic and abiotic stresses in plants [7, 8, 30]. So far, the identification and functional analysis of the OPR gene family have been characterized in many plants, such as *Arabidopsis* (3), rice (12), tomato (4), maize (8), and wheat (48). However, the OPR gene family in cultivated peanut and its functional characterization have not been investigated. In this study, we constructed a rooted maximum likelihood (ML) phylogenetic tree with 20 peanut OPR genes in accordance with the phylogenetic relationships of two species, *Arabidopsis* and rice. Accordingly, the OPR gene family in peanut can be divided into two subfamilies (I and II). The number of *AhOPR* genes (9) is substantially higher compared to most diploid plants but lower than that of hexaploid wheat (48), which might be related to the fact that the allotetraploid genome of cultivated peanut has undergone whole-genome duplication and other gene duplication events [31,32]. There were six *AdOPR* genes in diploid peanut *A. duranensis* and five *AiOPR* genes in diploid peanut *A. ipaensis*, while the number of allotetraploid *AhOPR* genes was less than the sum of two diploid OPR gene numbers. This phenomenon could be explained by reports that some homologous genes might have been lost or that some functionally redundant genes disappeared during the polyploidization of the genome [33,34].

Structure diversity within gene families was a mechanism for the evolution of many gene families. Intron gain and loss play a significant role in structural diversity and complexity. We found that most OPRs in peanut contain 3–5 exons; all the genes in OPR II contain 4 introns, while most OPRs (approximately 70%) in OPR I have 2–3 introns, and the others contain more than 4 introns. In wheat, the OPR genes in subfamilies I, II, IV, and V contain 3–5 introns; 29 of 32 OPR genes in subfamily III contain 1–2 introns. In addition,

subfamily III was the youngest subfamily in wheat which possessed the fewest introns [15]. The result was consistent with a previous study showing that the intron loss events occurred during the structural evolution of the *OPR* gene family [14]. Analogously, four of six maize *OPR* genes in subgroup I (*ZmOPR1-6*) contain 0–1 introns; the other two genes in subgroup II (*ZmOPR7* and *ZmOPR8*) have 3 or 4 introns [19]. The above results indicate that intron loss events could be found in different plants, whether dicots or monocots. All peanut *OPRs* in subfamilies I and II had motif 1, motif 2, motif 3, motif 5, and motif 7. These five motifs were related to the most conserved domains of *OPRs* and were associated with the alpha or beta barrel of protein secondary structures. Interestingly, the position of motif 9 of three genes (*AiOPR3*, *AiOPR5*, and *AdOPR3*) was replaced with motif 4. Four *OPRs* in OPRII lacked motif 8, which would impact the $\beta 6$ barrel of the protein secondary structures. Structural integrity is essential to ensuring gene function, and slight alterations in the DNA structure or protein motifs usually affect gene functions [35,36].

Cis-acting elements are found in the promoter regions upstream of protein-coding genes, and they are transcription factor (TF) binding sites. TFs and cis-acting elements interact to control the precise initiation of gene transcription, resulting in tissue-specific and signal-specific gene expression [37]. Many cis-acting elements related to growth and development (such as endosperm and meristem development), hormones (including MeJA, ABA, SA, GA, and auxin), and stresses (such as drought, zein metabolism, low-temperature, circadian, anaerobic, and defense responses) have been identified in peanut *OPR* promoters. Among hormone-responsive elements, MeJA responsiveness cis-acting elements (TGACG-motif and CGTCA-motif) were the most abundant, followed by ABA-responsive element ABRE, SA-responsive TCA element, and the auxin-responsive TGA element. Moreover, MeJA responsiveness has been demonstrated to be linked to plant defense mechanisms [38]. Therefore, we can infer the function of peanut *OPR* genes through the cis-acting elements in the gene promoter, which offered an efficient method for screening potential candidate genes.

The stationary nature of plants makes them susceptible to a variety of stresses, and peanut is no exception. Various abiotic stresses and biotic stresses, like stress caused by salinity, drought, cold, heat, and herbivores, adversely impact staple food crops' survival, biomass production, and yield by up to 70% [39–41]. According to recent research, drought affects approximately 45% of all agricultural land in the world, while salt impacts about 19.5% of it [42]. In accordance with the FAO's estimates, salinity affects over 6% of the world's land [41]. According to recent studies, *OPRs* were positively regulated in *Arabidopsis*, maize, and wheat when exposed to salt stress [22,43]. In maize, the overexpression of *ZmOPR1* affected *RD22*, *RD29B*, and *ABF2*, which are genes associated with osmotic and NaCl stresses [43]. *RD22* and *RD29B* are ABA-responsive genes; *ABF2* belongs to the ABF subfamily of bZIP proteins that interact with ABA-responsive elements. They are involved in ABA/stress responses [44–46]. Likewise, wheat *OPR1* could be induced by ABA and salinity, and the inhibition of ABA synthesis largely counteracts salinity-induced *TaOPR1* accumulation. As a result, there is a convincing argument that *TaOPR1* expression is induced by ABA synthesis. *AtRD22*, *AtRD29A*, and *AtRD29B* are all upregulated via an ABA-induced signaling cascade [47]. As a result of *TaOPR1* expression, *AtNCED3* and *AtAAC3*, which encode enzymes essential for ABA synthesis, were also significantly increased in transcript abundance. *AtMYB2*, an R2R3-MYB transcription factor gene, was induced by ABA, dehydration, and salt stresses [48,49], indicating that *AtMYB2* responds to environmental stresses through ABA-dependent and ABA-independent pathways [50,51]. Aside from *AtMYB2*, *AtMYC2* also activates genes in the ABA signaling pathway [52,53]. It has been documented that *AtMYB2* and *AtMYC2* can bind to MYB and MYC recognition sites in the promoter sequence of the *rd22BP1* gene, respectively, to regulate the

expression of ABA-inducible genes (like *rd22*), thus enhancing transgenic plant stress resistance [53,54]. The expression of *AhOPR6* markedly increased the transcript abundance of *AtAAO3*, *AtNCED3*, *AtRD22*, *AtRD29A*, *AtRD29B*, *AtMYB2*, and *AtMYC2* (Figure 10). The above investigations provide firm evidence that *AhOPR6* plays a positive role in salt stress through ABA-dependent signaling pathways.

There are several factors that lead to salt stress on plants, including ion toxicity [55], osmotic stress [56], and reactive oxygen species (ROS) [57]. Salt stress leads to the accumulation of ROS such as superoxide, H₂O₂, and hydroxyl radicals; oxidative damage and ROS accumulation are both increased with prolonged salt stress exposure [58]. Similarly, other studies supported our results, indicating that significantly higher antioxidant enzyme activity reduced ROS production and led to improved osmotic adaptation to salt stress [59]. POD plays an important role in ROS signaling and redox reactions, and a high level of POD can increase plants' salt tolerance [60]. In addition, the activities of POD and CAT were increased to reduce ROS accumulation under salt stress [61], and this result is consistent with our research. MDA, a product of membrane peroxidation, is often used as a prime indicator of oxidative stress in salt-stressed tissues [62,63]. Salt-sensitive plants exhibit a greater amount of MDA than salt-tolerant ones [64]. In our study, the decrease in MDA contents in *AtOE* lines implied that the overexpression of *AhOPR6* increased the plants' salt tolerance mainly by reducing ROS damage.

JA and its intermediates are critical elements of perception and signaling, and JA-mediated gene expression and signaling pathways can be triggered by several corroborative receptors, activators, transcription factors, repressors, and co-repressors [8,10]. In the first half of JA biosynthesis, *LOX*, *AOS*, and *AOC* sequentially catalyze to generate the intermediate product *cis-(+)-OPDA* [65]. The expression levels of *AtOPR3* and *AtJAZ1* (receptor genes of JA) were unchanged (Figure 10); these results indicate that JA synthesis in OE lines does not depend on *AhOPR6*. Through *AtMYC2*, the JA-activated MKK3-MPK6 signal negatively regulates the JA pathway and affects JA-dependent gene expression [66]. It is worth noting that the bHLH transcription factor *AtMYC2*, activated by JA, significantly interacts with the signaling pathways of ABA, JA, GA, and ethylene [67]. We found that the expression level of *AtMYC2* was increased, but *AtJAZ1* was unchanged in *AtOE-AhOPR6* lines. These results could be attributed to the promotion of ABA but not the JA signaling pathway, and it is highly possible that *AhOPR6* was not regulating JA synthesis (Figure 11). The research conducted by Dong et al. also verified our hypothesis [22] that the OPR1 (*TaOPR1*) gene exerts no regulatory activity on JA synthesis and JA signaling pathways.

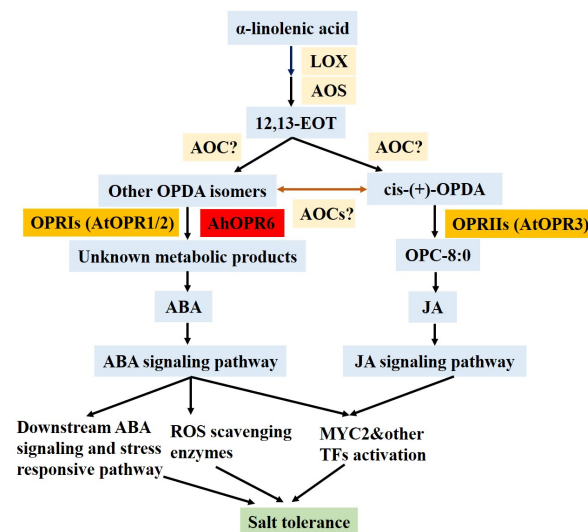


Figure 11. Salt stress signal and regulatory mechanism of *AhOPR6*.

4. Materials and Methods

4.1. Identification of Peanut OPR Gene Family Members

The protein sequence, gene annotation information file (gff3), and coding sequence (CDS) of the newly published peanut genome were obtained from the PeanutBase database (<https://www.peanutbase.org/>, accessed on 21 January 2022). The Hidden Markov model of the OPR gene family (PF00724) was downloaded from the Pfam database (<https://pfam.xfam.org/>, accessed on 5 May 2025) [68], and then this profile was used to search the peanut protein database with E-values $< 1.2 \times 10^{-28}$ by HMMER 3.0. The protein sequence of OPRs was extracted via Perl language and submitted to the web tools SMART (<http://smart.embl.de/smart/batch.pl>, accessed on 5 May 2025), Pfam (<https://pfam.xfam.org/search>, accessed on 5 May 2025), and NCBI-CDD (<https://www.ncbi.nlm.nih.gov/cdd/>, accessed on 5 May 2025) to verify the structural integrity of OPR. Finally, reliable OPR candidate genes were determined. The molecular weight (MW), amino acid sequence length (aa), and isoelectric point (pI) of the OPR were predicted using the online server ExPASy (<https://web.expasy.org/cgi-bin/protparam/protparam>, accessed on 5 May 2025) [69]. Subcellular localization of OPRs was predicted using the online web tool WoLF PSORT (<https://wolfpsort.hgc.jp/>, accessed on 5 May 2025).

4.2. Phylogenetic Analysis

To further understand the evolutionary relationship of the OPR gene family, 3 *Arabidopsis* OPRs and 11 rice OPRs amino acid sequences were downloaded from the NCBI database, and 20 peanut OPRs were downloaded from PeanutBase (<https://www.peanutbase.org/>, accessed on 5 May 2025). The multiple sequence alignment of amino acid sequences was conducted via the ClustalW function of MEGA X software, and the phylogenetic relationships of the three species were constructed using the neighbor-joining method; the bootstrap value was set to 1000. The classifications of OPRs in peanut were based on the topological structure of the phylogenetic tree and sequence similarity. The established phylogenetic trees were beautified using Evolview (<http://www.evolgenius.info/evolview/>, accessed on 5 May 2025) [70].

4.3. Analysis of Gene Structure and Protein Conserved Domains of OPRs

Based on peanut genome annotation information, location information of the exon, intron, and UTR of OPR genes on chromosomes was obtained, which was used to draw gene structure. Conserved motifs with lengths of 6–100 aa in 20 OPR proteins were analyzed using the MEME (<https://meme-suite.org/meme/tools/meme>, accessed on 5 May 2025) program [71]. The maximum number of motifs was set at 10. The gene structure and conserved motifs of OPRs were visualized using TBtoolsV1.098 software [72].

4.4. Cis-Acting Regulatory Elements and Gene Ontology (GO) Annotation

The 2 kb promoter sequence of OPRs was extracted from peanut genomic DNA sequences of the PeanutBase database and uploaded to PlantCARE (<http://bioinformatics.psb.ugent.be/webtools/plantcare/html/>, accessed on 5 May 2025) [73] to predict cis-acting regulatory elements in the promoter region. The GO analysis was conducted in the ShinyGO 0.80 database (<http://bioinformatics.sdstate.edu/go/>, accessed on 5 May 2025) by inputting all OPR family genes to ascertain the molecular functions, biological processes, and cell components related to peanut OPRs [74].

4.5. Chromosome Localization and Synteny Analysis

To determine the distribution of OPRs on chromosomes, we obtained the starting and ending positions of OPR genes from peanut genome annotation files (gff3) and submitted

their location information to the online tool MapGene2Chrom web v2 (http://mg2c.iask.in/mg2c_v2.0/, accessed on 5 May 2025) to map their chromosome positions. The segmental and tandem repeats of *OPR* family members in peanut were analyzed via MCScanX (<http://chibba.pgml.uga.edu/mcscan2/>, accessed on 5 May 2025) software [75]. Two adjacent genes located on the same chromosome with a relative position less than 100 kb are defined as tandem repeat genes [76]. The chromosome distribution of 20 *OPR* genes and the collinearity of related genes were plotted by using Circos (version 0.69) software [77].

4.6. RNA-Seq Data Analysis of *OPRs*

The expression patterns of *OPR* genes in different tissues and different stress treatments were investigated in peanut. In this study, RNA-seq data of 22 tissues were derived from the PeanutBase database [78], and the FPKM values of drought [79] and salt [80] stresses were obtained from our previous work. The PFKM values of *OPR* family genes were standardized by log₂ PFKM, and the heatmap was drawn using Heml_1.0 software.

4.7. Subcellular Localization of *AhOPR6* Protein

The coding sequences of *AhOPR3* and *AhOPR6* were amplified from peanut cultivar “huayu71” and used to construct the 35S::*AhOPR3*-GFP and 35S::*AhOPR6*-GFP fusion vectors. The empty vector and the two fusion vectors were transiently expressed in *Nicotiana benthamiana* leaves. After three days, a confocal microscope (TCS-SP8, Leica, Wetzlar, Germany) was used to observe the fluorescence signals of the fusion proteins in the cells.

4.8. Construction of *AhOPR6* Vectors and Generation of Transgenic *Arabidopsis* Plants

Full-length coding sequence of *AhOPR6* was amplified from the cDNA of peanut cultivar “huayu71” by PCR. To construct the overexpression vector, the *AhOPR6* gene was placed between the 35S promoter and the Nos terminator in the pCambia2300EC vector. The recombinant plasmid was transformed into *Agrobacterium* strain GV3101, which was then applied in floral dipping to transform wild-type *Arabidopsis*. Positive seedlings were derived from the selective media after being grown on MS media with 50 mg/l kanamycin, and T3 homozygous seedlings were employed for subsequent analysis.

4.9. The Treatment and Determination of Salt-Related Physiological Parameters in Transgenic *Arabidopsis*

Both WT and transgenic *Arabidopsis* seedlings were grown on 1/2 MS media for 7 days and then transferred to soil for 2 weeks. For salt stress, *Arabidopsis* seedlings were treated with 300 mM NaCl for one week. The malondialdehyde (MDA) content, superoxide dismutase (SOD), peroxidase (POD), and catalase (CAT) enzyme activities were detected using assay kits (Comin, Suzhou, China) for both overexpressing lines and WT *Arabidopsis*. The four physiological parameters of the *Arabidopsis* plants were measured in triplicate.

4.10. RNA Isolation and Real-Time Quantitative PCR (qRT-PCR) Validation of *OPR*

Trizol reagent (TaKaRa, Dalian, China) was used to extract total RNA from leaves of *Arabidopsis* under salt stress treatments. The integrity and quality of RNA were detected using 1% agarose gel electrophoresis, and the concentrations of RNA, namely OD₂₆₀/280 and OD₂₆₀/230, were detected using the Nanodrop one micro-ultraviolet spectrophotometer. Total RNA was reverse-transcribed into cDNA using the Transcriptor First Strand cDNA Synthesis Kit (TaKaRa, Dalian) and stored at −20 °C. qRT-PCR was performed on ABI7500 (Applied Biosystems, Foster City, CA, USA). The reaction system was as follows: 10 µL of 2×UltraSYBR Mixture, 0.4 µL of forward primer (5.0 µmol/L), 0.4 µL of reverse primer (5.0 µmol/L), 1 µL of cDNA (200 ng), and 7.4 µL of RNase-free water. The amplification

procedure was as follows: 95 °C for 5 min, 40 cycles of 95 °C for 10 s, and 60 °C for 1 min; 95 °C for 15 s, 60 °C for 1 min, 95 °C for 15 s, and 60 °C for 15 s. Three biological repeats and three technical repeats were set up in each treatment. The relative expression of genes was calculated using $2^{-\Delta\Delta C_t}$ [81]. The fluorescent quantitative primers were designed using Primer-BLAST (<https://www.ncbi.nlm.nih.gov/tools/primer-blast/index.cgi>, accessed on 5 May 2025).

5. Conclusions

In this study, a total of 20 *OPR* genes were identified in the genome of a tetraploid cultivar and two diploid peanut species. They were divided into two subfamilies with *Arabidopsis* and rice homologous genes. The investigation of the evolutionary relationship, gene structure, protein conserved motifs, chromosome locations, gene duplication, tissue expression patterns, and expression patterns under salt and drought stresses indicated their diversity in different *OPR* genes. The subcellular location of peanut *AhOPR3* and *AhOPR6* revealed that they were distributed on the plasma membranes and localized in the chloroplast, respectively. Furthermore, the overexpression of *AhOPR6* in *Arabidopsis* increased tolerance to salt stress. Notably, the detection of JA and ABA signaling pathway-related genes by qRT-PCR indicated that *AhOPR6* might enhance salt stress tolerance through an ABA-dependent pathway. Overall, we constructed a hypothetical model of *AhOPR6*'s action in improving salt tolerance and provided candidate *OPR* genes for further functional studies in growth and development, as well as peanut stress resistance breeding.

Supplementary Materials: The following supporting information can be downloaded at <https://www.mdpi.com/article/10.3390/plants14101408/s1>. Table S1: Characteristics of putative peanut *OPR* genes; Table S2: Detailed information about conserved motifs of *AhOPRs*; Table S3: Tandem and segmentally duplicated *OPR* gene pairs in peanut; Table S4: Analysis of cis-acting regulatory elements of peanut *OPR* promoters; Table S5: FPKM values of peanut *OPR* genes under two abiotic stresses (drought and salt) in this study; Table S6: FPKM values of peanut *OPR* genes in 22 tissues in this study; Table S7: Primer sequences used in this study; Figure S1: Three-dimensional structure prediction of peanut *OPRs*.

Author Contributions: Y.M. conceived and designed the study. Y.M. performed the experiments and wrote the manuscript. Q.S., H.M., J.W. and Q.W. (Qi Wang) analyzed the bioinformatics data. Q.W. (Qianqian Wang), C.Y. (Caixia Yan), C.Y. (Cuiling Yuan) and X.Z. assisted in the stress treatment and data analysis. S.S. and C.L. revised the paper. All authors have read and agreed to the published version of the manuscript.

Funding: This research was funded by the Qingdao Natural Science Foundation (grant number: 23-2-1-44-zyyd-jch), the National Key Research, Development Program of China (grant number: 2022YFD1200403), the Agro-industry Technology Research System of Shandong Province (grant number: SDAIT-04-01), the Key research and development project of Shandong province (grant number: 2024LZGC031), and the Innovation Project of SAAS (grant number: CXGC2024D19), Tianchi talent program.

Data Availability Statement: The original contributions presented in this study are included in the article/supplementary material. Further inquiries can be directed to the corresponding author(s).

Conflicts of Interest: The authors declare no conflicts of interest.

References

1. Zhang, H.; Tang, Y.; Yue, Y.; Chen, Y. Advances in the evolution research and genetic breeding of peanut. *Gene* **2024**, *916*, 148425. [[CrossRef](#)]
2. Dwivedi, S.L.; Crouch, J.H.; Nigam, S.N.; Ferguson, M.E.; Paterson, A.H. Molecular breeding of groundnut for enhanced productivity and food security in the semi- arid tropics: Opportunities and challenges. *Adv. Agron.* **2003**, *80*, 153–221.

3. Sarkar, T.; Thankappan, R.; Kumar, A.; Mishra, G.P.; Dobarra, J.R.; Zhang, J.S. Heterologous Expression of the *AtDREB1A* Gene in Transgenic Peanut—Conferred Tolerance to Drought and Salinity Stresses. *PLoS ONE* **2014**, *9*, e110507. [[CrossRef](#)] [[PubMed](#)]
4. Abrol, I.P.; Yadav, J.S.P.; Massoud, F.I. *Salt-Affected Soils and Their Management*; Food and Agriculture Organization of the United Nations: Rome, Italy, 1988.
5. Yang, S.; Hao, X.; Xu, Y.; Yang, J.; Su, D. Meta-Analysis of the Effect of Saline-Alkali Land Improvement and Utilization on Soil Organic Carbon. *Life* **2022**, *12*, 1870. [[CrossRef](#)] [[PubMed](#)]
6. Liu, Y.; Zhu, J.; Sun, S.; Cui, F.; Han, Y.; Peng, Z.; Zhang, X.; Wan, S.; Li, G. Defining the function of SUMO system in pod development and abiotic stresses in Peanut. *BMC Plant Biol.* **2019**, *19*, 593. [[CrossRef](#)] [[PubMed](#)]
7. Turner, J.G.; Ellis, C.; Devoto, A. The jasmonate signal pathway. *Plant Cell* **2002**, *14*, S153–S164. [[CrossRef](#)]
8. Wasternack, C.; Hause, B. Jasmonates: Biosynthesis, perception, signal transduction and action in plant stress response, growth and development. An update to the 2007 review in *Annals of Botany*. *Ann. Bot.* **2013**, *111*, 1021–1058. [[CrossRef](#)]
9. Wasternack, C. Jasmonates: An update on biosynthesis, signal transduction and action in plant stress response, growth and development. *Ann. Bot.* **2007**, *100*, 681–697. [[CrossRef](#)]
10. Wasternack, C.; Strnad, M. Jasmonate signaling in plant stress responses and development—Active and inactive compounds. *New Biotechnol.* **2016**, *33*, 604–613. [[CrossRef](#)]
11. Huang, H.; Liu, B.; Liu, L.; Song, S. Jasmonate action in plant growth and development. *J. Exp. Bot.* **2017**, *68*, 1349–1359. [[CrossRef](#)]
12. Li, W.; Liu, B.; Yu, L.; Feng, D.; Wang, H.; Wang, J. Phylogenetic analysis, structural evolution and functional divergence of the 12-oxo-phytyldienoate acid reductase gene family in plants. *Bmc Evol. Biol.* **2009**, *9*, 90. [[CrossRef](#)]
13. Breithaupt, C.; Kurzbauer, R.; Schaller, F.; Stintzi, A.; Schaller, A.; Huber, R.; Macheroux, P.; Clausen, T. Structural Basis of Substrate Specificity of Plant 12-Oxophytyldienoate Reductases. *J. Mol. Biol.* **2009**, *392*, 1266–1277. [[CrossRef](#)]
14. Li, W.; Zhou, F.; Liu, B.; Feng, D.; He, Y.; Qi, K.; Wang, H.; Wang, J. Comparative characterization, expression pattern and function analysis of the 12-oxo-phytyldienoic acid reductase gene family in rice. *Plant Cell Rep.* **2011**, *30*, 981–995. [[CrossRef](#)] [[PubMed](#)]
15. Mou, Y.; Liu, Y.; Tian, S.; Guo, Q.; Wen, S. Genome-Wide Identification and Characterization of the *OPR* Gene Family in Wheat (*Triticum aestivum* L.). *Int. J. Mol. Sci.* **2019**, *20*, 1914. [[CrossRef](#)] [[PubMed](#)]
16. Schaller, F.; Weiler, E.W. Molecular cloning and characterization of 12-oxophytyldienoate reductase, an enzyme of the octadecanoid signaling pathway from *Arabidopsis thaliana*—Structural and functional relationship to yeast old yellow enzyme. *J. Biol. Chem.* **1997**, *272*, 28066–28072. [[CrossRef](#)]
17. Schaller, F.; Biesgen, C.; Mussig, C.; Altmann, T.; Weiler, E.W. 12-oxophytyldienoate reductase 3 (*OPR3*) is the isoenzyme involved in jasmonate biosynthesis. *Planta* **2000**, *210*, 979–984. [[CrossRef](#)]
18. Biesgen, C.; Weiler, E.W. Structure and regulation of *OPR1* and *OPR2*, two closely related genes encoding 12-oxophytyldienoic acid-10,11-reductases from *Arabidopsis thaliana*. *Planta* **1999**, *208*, 155–165. [[CrossRef](#)] [[PubMed](#)]
19. Zhang, J.; Simmons, C.; Yalpani, N.; Crane, V.; Wilkinson, H.; Kolomiets, M. Genomic Analysis of the 12-oxo-phytyldienoic Acid Reductase Gene Family of *Zea mays*. *Plant Mol. Biol.* **2005**, *59*, 323–343. [[CrossRef](#)]
20. Scalschi, L.; Sanmartin, M.; Camanes, G.; Troncho, P.; Sanchez-Serrano, J.J.; Garcia-Agustin, P.; Vicedo, B. Silencing of *OPR3* in tomato reveals the role of OPDA in callose deposition during the activation of defense responses against *Botrytis cinerea*. *Plant J.* **2015**, *81*, 304–315. [[CrossRef](#)]
21. Strassner, J.; Fürholz, A.; Macheroux, P.; Amrhein, N.; Schaller, A. A homolog of old yellow enzyme in tomato. Spectral properties and substrate specificity of the recombinant protein. *J. Biol. Chem.* **1999**, *274*, 35067–35073. [[CrossRef](#)]
22. Dong, W.; Wang, M.; Xu, F.; Quan, T.; Peng, K.; Xiao, L.; Xia, G. Wheat Oxophytyldienoate Reductase Gene *TaOPR1* Confers Salinity Tolerance via Enhancement of Abscisic Acid Signaling and Reactive Oxygen Species Scavenging. *Plant Physiol.* **2013**, *161*, 1217–1228. [[CrossRef](#)]
23. Yan, Y.; Christensen, S.; Isakeit, T.; Engelberth, J.; Meeley, R.; Hayward, A.; Emery, R.J.N.; Kolomiets, M.V. Disruption of *OPR7* and *OPR8* Reveals the Versatile Functions of Jasmonic Acid in Maize Development and Defense. *Plant Cell* **2012**, *24*, 1420–1436. [[CrossRef](#)] [[PubMed](#)]
24. Guo, H.-M.; Li, H.-C.; Zhou, S.-R.; Xue, H.-W.; Miao, X.-X. Cis-12-Oxo-Phytyldienoic Acid Stimulates Rice Defense Response to a Piercing-Sucking Insect. *Mol. Plant* **2014**, *7*, 1683–1692. [[CrossRef](#)] [[PubMed](#)]
25. Bosch, M.; Wright, L.P.; Gershenzon, J.; Wasternack, C.; Hause, B.; Schaller, A.; Stintzi, A. Jasmonic Acid and Its Precursor 12-Oxophytyldienoic Acid Control Different Aspects of Constitutive and Induced Herbivore Defenses in Tomato. *Plant Physiol.* **2014**, *166*, 396–410. [[CrossRef](#)] [[PubMed](#)]
26. Stintzi, A.; Browse, J. The *Arabidopsis* male-sterile mutant, *OPR3*, lacks the 12-oxophytyldienoic acid reductase required for jasmonate synthesis. *Proc. Natl. Acad. Sci. USA* **2000**, *97*, 10625–10630. [[CrossRef](#)]
27. Li, S.; Ma, J.; Liu, P. *OPR3* is expressed in phloem cells and is vital for lateral root development in *Arabidopsis*. *Can. J. Plant Sci.* **2013**, *93*, 165–170. [[CrossRef](#)]

28. Wang, Y.; Yuan, G.; Yuan, S.; Duan, W.; Wang, P.; Bai, J.; Zhang, F.; Gao, S.; Zhang, L.; Zhao, C. *TaOPR2* encodes a 12-oxo-phytyldienoic acid reductase involved in the biosynthesis of jasmonic acid in wheat (*Triticum aestivum* L.). *Biochem. Biophys. Res. Commun.* **2016**, *470*, 233–238. [[CrossRef](#)]
29. Ren, W.; Chen, L.; Xie, Z.M.; Peng, X. Combined transcriptome and metabolome analysis revealed pathways involved in improved salt tolerance of *Gossypium hirsutum* L. seedlings in response to exogenous melatonin application. *BMC Plant Biol.* **2022**, *22*, 552. [[CrossRef](#)]
30. Tani, T.; Sobajima, H.; Okada, K.; Chujo, T.; Arimura, S.I.; Tsutsumi, N.; Nishimura, M.; Seto, H.; Nojiri, H.; Yamane, H. Identification of the *OsOPR7* gene encoding 12-oxophytyldienoate reductase involved in the biosynthesis of jasmonic acid in rice. *Planta* **2008**, *227*, 517–526. [[CrossRef](#)]
31. Bertoli, D.J.; Cannon, S.B.; Froenicke, L.; Huang, G.; Farmer, A.D.; Cannon, E.K.; Liu, X.; Gao, D.; Clevenger, J.; Dash, S.; et al. The genome sequences of *Arachis duranensis* and *Arachis ipaensis*, the diploid ancestors of cultivated peanut. *Nat. Genet.* **2016**, *48*, 438–446. [[CrossRef](#)]
32. Bertoli, D.J.; Seijo, G.; Freitas, F.O.; Valls, J.; Leal-Bertoli, S.; Moretzsohn, M.C. An overview of peanut and its wild relatives. *Plant Genet. Resour.* **2011**, *9*, 134–149. [[CrossRef](#)]
33. Lynch, M.; Force, A. The probability of duplicate gene preservation by subfunctionalization. *Genetics* **2000**, *154*, 459. [[CrossRef](#)] [[PubMed](#)]
34. Ma, X.; Ai, X.; Li, C.; Wang, S.; Zhang, N.; Ren, J.; Wang, J.; Zhong, C.; Zhao, X.; Zhang, H.; et al. A Genome-Wide Analysis of the Jasmonic Acid Biosynthesis Gene Families in Peanut Reveals Their Crucial Roles in Growth and Abiotic Stresses. *Int. J. Mol. Sci.* **2024**, *25*, 7054. [[CrossRef](#)]
35. Yan, L.; Zhang, J.; Chen, H.; Luo, H. Genome-wide analysis of ATP-binding cassette transporter provides insight to genes related to bioactive metabolite transportation in *Salvia miltiorrhiza*. *BMC Genom.* **2021**, *22*, 315. [[CrossRef](#)] [[PubMed](#)]
36. Nyland, J.; Silbergeld, E. A nanobiological approach to nanotoxicology. *Hum. Exp. Toxicol.* **2009**, *28*, 393. [[CrossRef](#)]
37. Carlberg, C.; Molnár, F. *Mechanisms of Gene Regulation: How Science Works*; Springer: Berlin/Heidelberg, Germany, 2020.
38. Motallebi, P.; Niknam, V.; Ebrahimzadeh, H.; Enferadi, S.T.; Hashemi, M. The effect of methyl jasmonate on enzyme activities in wheat genotypes infected by the crown and root rot pathogen *Fusarium culmorum*. *Acta Physiol. Plant.* **2015**, *37*, 237. [[CrossRef](#)]
39. Mantri, N.; Patade, V.; Penna, S.; Ford, R.; Pang, E. Abiotic stress responses in plants: Present and future. In *Abiotic Stress Responses in Plants*; Springer: New York, NY, USA, 2012.
40. Ahmad, P. Salt-induced changes in photosynthetic activity and oxidative defense system of three cultivars of mustard (*Brassica juncea* L.). *Afr. J. Biotechnol.* **2012**, *11*, 2694–2703.
41. Parihar, P.; Singh, S.; Singh, R.; Singh, V.P.; Prasad, S.M. Effect of salinity stress on plants and its tolerance strategies: A review. *Environ. Sci. Pollut. Res.* **2015**, *22*, 4056–4075. [[CrossRef](#)]
42. Hossain, A.; Khrupnick, T.; Timsina, J.; Mahboob, M.G.; Hasanuzzaman, M. Agricultural Land Degradation: Processes and Problems Undermining Future Food Security. In *Environment, Climate, Plant and Vegetation Growth*; Springer: Cham, Switzerland, 2020.
43. Gu, D.; Liu, X.; Wang, M.; Zheng, J.; Hou, W.; Wang, G.; Wang, J. Overexpression of *ZmOPR1* in *Arabidopsis* enhanced the tolerance to osmotic and salt stress during seed germination. *Plant Sci.* **2008**, *174*, 124–130. [[CrossRef](#)]
44. Kim, S.; Kang, J.y.; Cho, D.I.; Park, J.H.; Kim, S.Y. *ABF2*, an ABRE-binding bZIP factor, is an essential component of glucose signaling and its overexpression affects multiple stress tolerance. *Plant J.* **2004**, *40*, 75–87. [[CrossRef](#)]
45. Yu, D.; Li, X.; Zhao, X.; Du, C.; Chen, J.; Li, C.; Sun, M.; Wang, L.; Lin, J.; Tang, D. *RPN1a* negatively regulates ABA signaling in *Arabidopsis*. *Plant Physiol. Biochem. PPB* **2016**, *108*, 279–285. [[CrossRef](#)]
46. Gao, F.; Yao, H.; Zhao, H.; Zhou, J.; Luo, X.; Huang, Y.; Li, C.; Chen, H.; Wu, Q. Tartary buckwheat *FtMYB10* encodes an R2R3-MYB transcription factor that acts as a novel negative regulator of salt and drought response in transgenic *Arabidopsis*. *Plant Physiol. Biochem.* **2016**, *109*, 387–396. [[CrossRef](#)] [[PubMed](#)]
47. Fujita, Y.; Fujita, M.; Shinozaki, K.; Yamaguchi-Shinozaki, K. ABA-mediated transcriptional regulation in response to osmotic stress in plants. *J. Plant Res.* **2011**, *124*, 509–525. [[CrossRef](#)] [[PubMed](#)]
48. Abe, H. Role of *Arabidopsis* MYC and MYB Homologs in Drought and Abscisic Acid-Regulated Gene Expression. *Plant Cell* **1997**, *9*, 1859–1868.
49. Zhu, S.; Shi, W.; Jie, Y.; Zhou, Q.; Song, C. A MYB transcription factor, *BnMYB2*, cloned from ramie (*Boehmeria nivea*) is involved in cadmium tolerance and accumulation. *PLoS ONE* **2020**, *15*, e0233375. [[CrossRef](#)] [[PubMed](#)]
50. Urao, T. An *Arabidopsis myb* homolog is induced by dehydration stress and its gene product binds to the conserved MYB recognition sequence. *Plant Cell* **1993**, *5*, 1529–1539.
51. Zhao, P.; Hou, S.; Guo, X.; Jia, J.; Yang, W.; Liu, Z.; Chen, S.; Li, X.; Qi, D.; Liu, G. A MYB-related transcription factor from sheepgrass, *LcMYB2*, promotes seed germination and root growth under drought stress. *BMC Plant Biol.* **2019**, *19*, 564. [[CrossRef](#)]
52. Li, L.; Yu, X.; Thompson, A.; Guo, M.; Yoshida, S.; Asami, T.; Chory, J.; Yin, Y. *Arabidopsis* MYB30 is a direct target of *BES1* and cooperates with *BES1* to regulate brassinosteroid-induced gene expression. *Plant J.* **2010**, *58*, 275–286. [[CrossRef](#)]

53. Hiroshi, A.; Takeshi, U.; Takuya, I.; Motoaki, S.; Kazuo, S. Arabidopsis *AtMYC2* (*bHLH*) and *AtMYB2* (MYB) Function as Transcriptional Activators in Abscisic Acid Signaling. *Plant Cell* **2003**, *15*, 63–78.
54. Liang, X.; Li, Y.; Yao, A.; Liu, W.; Yang, T.; Zhao, M.; Zhang, B.; Han, D. Overexpression of *MxbHLLH18* Increased Iron and High Salinity Stress Tolerance in *Arabidopsis thaliana*. *Int. J. Mol. Sci.* **2022**, *23*, 8007. [[CrossRef](#)]
55. Flowers, T.J.; Rana, M.; Colmer, T.D. Sodium chloride toxicity and the cellular basis of salt tolerance in halophytes. *Ann. Bot.* **2015**, *115*, 419–431. [[CrossRef](#)] [[PubMed](#)]
56. Begum, N.; Hasanuzzaman, M.; Li, Y.; Akhtar, K.; Zhang, C.; Zhao, T. Seed Germination Behavior, Growth, Physiology and Antioxidant Metabolism of Four Contrasting Cultivars under Combined Drought and Salinity in Soybean. *Antioxidants* **2022**, *11*, 498. [[CrossRef](#)]
57. Liya, M.; Huan, Z.; Lirong, S.; Yiheng, J.; Guozeng, Z.; Chen, M.; Fushun, H. NADPH oxidase *AtrbohD* and *AtrbohF* function in ROS-dependent regulation of Na/Khomeostasis in Arabidopsis under salt stress. *J. Exp. Bot.* **2012**, *63*, 305–317.
58. Xie, Q.; Niu, J.; Xu, X.; Xu, L.; Zhang, Y.; Fan, B.; Liang, X. De novo assembly of the Japanese lawngress (*Zoysia japonica* Steud.) root transcriptome and identification of candidate unigenes related to early responses under salt stress. *Front. Plant Sci.* **2015**, *6*, 610.
59. Chang, B.; Ma, K.; Lu, Z.; Lu, J.; Cui, J.; Wang, L.; Jin, B. Physiological, Transcriptomic, and Metabolic Responses of *Ginkgo biloba* L. to Drought, Salt, and Heat Stresses. *Biomolecules* **2020**, *10*, 1635. [[CrossRef](#)]
60. Chen, F.; Fang, P.; Peng, Y.; Zeng, W.; Zhao, X.; Ding, Y.; Zhuang, Z.; Gao, Q.; Ren, B. Comparative Proteomics of Salt-Tolerant and Salt-Sensitive Maize Inbred Lines to Reveal the Molecular Mechanism of Salt Tolerance. *Int. J. Mol. Sci.* **2019**, *20*, 4725. [[CrossRef](#)]
61. Xu, L.; Song, J.Q.; Wang, Y.L.; Liu, X.H.; Li, X.L.; Zhang, B.; Li, A.J.; Ye, X.F.; Wang, J.; Wang, P. Thymol improves salinity tolerance of tobacco by increasing the sodium ion efflux and enhancing the content of nitric oxide and glutathione. *BMC Plant Biol.* **2022**, *22*, 31. [[CrossRef](#)]
62. Mir, M.A.; John, R.; Alyemeni, M.N.; Alam, P.; Ahmad, P. Jasmonic acid ameliorates alkaline stress by improving growth performance, ascorbate glutathione cycle and glyoxylase system in maize seedlings. *Sci. Rep.* **2018**, *8*, 2831. [[CrossRef](#)]
63. El-Beltagi, H.S.; Salama, Z.A.; El Hariri, D.M. Some Biochemical Markers for Evaluation of Flax Cultivars Under Salt Stress Conditions. *J. Nat. Fibers* **2008**, *5*, 316–330. [[CrossRef](#)]
64. Koca, H.; Bor, M.; Zdemir, F.; Turkan, I. The effect of salt stress on lipid peroxidation, antioxidative enzymes and proline content of sesame cultivars. *Environ. Exp. Bot.* **2007**, *60*, 344–351. [[CrossRef](#)]
65. Claus, W.; Bettina, H. A Bypass in Jasmonate Biosynthesis—The *OPR3*-independent Formation. *Trends Plant Sci.* **2018**, *23*, 276–279.
66. Takahashi, F.; Yoshida, R.; Ichimura, K.; Mizoguchi, T.; Seo, S.; Yonezawa, M.; Maruyama, K.; Yamaguchi-Shinozaki, K.; Shinozaki, K. The mitogen-activated protein kinase cascade *MKK3-MPK6* is an important part of the jasmonate signal transduction pathway in *Arabidopsis*. *Plant Cell* **2007**, *19*, 805–818. [[CrossRef](#)] [[PubMed](#)]
67. Hong, G.J.; Xue, X.Y.; Mao, Y.B.; Wang, L.J.; Chen, X.Y. *Arabidopsis MYC2* Interacts with *DELLA* Proteins in Regulating Sesquiterpene Synthase Gene Expression. *Plant Cell* **2012**, *24*, 2635–2648. [[CrossRef](#)]
68. El-Gebali, S.; Mistry, J.; Bateman, A.; Eddy, S.R.; Luciani, A.; Potter, S.C.; Qureshi, M.; Richardson, L.J.; Salazar, G.A.; Smart, A. The Pfam protein families database in 2019. *Nucleic Acids Res.* **2019**, *47*, D427–D432. [[CrossRef](#)]
69. Wilkins, M.R.; Gasteiger, E.; Bairoch, A.; Sanchez, J.C.; Hochstrasser, D.F. Protein Identification and Analysis Tools in the ExPASy Server. *Methods Mol. Biol.* **1999**, *112*, 531–552.
70. Zilong, H.; Huangkai, Z.; Shenghan, G.; Lercher, M.J.; Wei-Hua, C.; Songnian, H. Evolvview v2: An online visualization and management tool for customized and annotated phylogenetic trees. *Nucleic Acids Res.* **2016**, *44*, W236–W241.
71. Timothy, L.B.; Nadya, W.; Chris, M.; Wilfred, W.L. MEME: Discovering and analyzing DNA and protein sequence motifs. *Nucleic Acids Res.* **2006**, *34*, W369.
72. Chen, C.; Chen, H.; Zhang, Y.; Thomas, H.R.; Xia, R. TBtools: An Integrative Toolkit Developed for Interactive Analyses of Big Biological Data. *Mol. Plant* **2020**, *13*, 1194–1202. [[CrossRef](#)]
73. Lescot, M. PlantCARE, a database of plant cis-acting regulatory elements and a portal to tools for in silico analysis of promoter sequences. *Nucleic Acids Res.* **2002**, *30*, 325–327. [[CrossRef](#)]
74. Ge, S.X.; Jung, D.; Yao, R. ShinyGO: A graphical gene-set enrichment tool for animals and plants. *Oxf. Acad.* **2020**, *36*, 2628–2629. [[CrossRef](#)]
75. Wang, Y.; Tang, H.; Debarry, J.D.; Tan, X.; Li, J.; Wang, X.; Lee, T.-H.; Jin, H.; Marler, B.; Guo, H.; et al. MCScanX: A toolkit for detection and evolutionary analysis of gene synteny and collinearity. *Nucleic Acids Res.* **2012**, *40*, e49. [[CrossRef](#)] [[PubMed](#)]
76. Hu, L.; Liu, S.; Somers, D.J. Genome-wide analysis of the *MADS-box* gene family in cucumber. *Genome* **2012**, *55*, 245–256. [[CrossRef](#)]
77. Krzywinski, M.; Schein, J.; Birol, I.; Connors, J.; Gascoyne, R.; Horsman, D.; Jones, S.J.; Marra, M.A. Circos: An information aesthetic for comparative genomics. *Genome Res.* **2009**, *19*, 1639–1645. [[CrossRef](#)] [[PubMed](#)]
78. Josh, C.; Ye, C.; Brian, S.; Ozias-Akins, P. A Developmental Transcriptome Map for Allotetraploid *Arachis hypogaea*. *Front. Plant Sci.* **2016**, *7*, 1446.

79. Zhang, H.; Zhao, X.B.; Sun, Q.X.; Yan, C.X.; Wang, J.; Yuan, C.L.; Li, C.J.; Shan, S.H.; Liu, F.Z. Comparative transcriptome analysis reveals molecular defensive mechanism of *Arachis hypogaea* in response to salt stress. *Int. J. Genom.* **2020**, *10*, 6524093. [[CrossRef](#)]
80. Zhao, X.B.; Li, C.J.; Wan, S.B.; Zhang, T.T.; Yan, C.X.; Shan, S.H. Transcriptomic analysis and discovery of genes in the response of *Arachis hypogaea* to drought stress. *Mol. Biol. Rep.* **2018**, *45*, 119–131. [[CrossRef](#)]
81. Livak, K.J.; Schmittgen, T.D.L. Analysis of relative gene expression data using real-time quantitative PCR and the 2-DDCt method. *Methods* **2001**, *25*, 402–408. [[CrossRef](#)]

Disclaimer/Publisher’s Note: The statements, opinions and data contained in all publications are solely those of the individual author(s) and contributor(s) and not of MDPI and/or the editor(s). MDPI and/or the editor(s) disclaim responsibility for any injury to people or property resulting from any ideas, methods, instructions or products referred to in the content.